

纳米羟基磷灰石纳米管的一种简便制备方法及其 对溶液中重金属离子的吸附

邹雪艳^{1,2} 赵彦保^{*,1,3,4} 张治军^{*,1,2,4}

(¹ 河南大学纳米材料工程研究中心, 开封 475004)

(² 河南省土壤重金属污染监测与修复重点实验室, 济源 459000)

(³ 河南大学纳米杂化材料应用技术国家地方联合工程研究中心, 开封 475004)

(⁴ 纳米功能材料及其应用河南省协同创新中心, 开封 475004)

摘要: 采用简便的方法合成了 20~40 nm 长、56 m²·g⁻¹ 的比表面积的羟基磷灰石纳米管(HAP)。然后用制备的 HAP 纳米管在水溶液中同时吸附 Pb²⁺、Cd²⁺、Cu²⁺、Co²⁺、Ni²⁺、Zn²⁺和 Hg²⁺, 其具有高的吸附能力, 并能实现快速去除。此外, 制备的 HAP 纳米管对 7 种重金属离子的脱附率均小于 1%, 表现出较强的稳定性。实验数据采用 Langmuir 等温线模型和 Freundlich 等温线模型进行分析。2 个方程的应用结果表明, 吸附平衡最适合 Langmuir 模型, 单层饱和吸附能力为 958.28 mg·g⁻¹, 具有较好的吸附性能。通过能量色散 X 射线光谱(EDS)和 X 射线衍射(XRD)图进一步研究了吸附机理, 结果表明, 当溶液中 Pb²⁺离子数量足够时, 吸附机理为 Pb 取代了 HAP 中的 Ca, 形成了更稳定的 Pb₅(PO₄)₃(OH)。上述实验研究预测了利用 HAP 纳米管处理含铅废水在环境污染治理中的可行性。

关键词: 羟基磷灰石; 纳米管; 吸附; 机理; 重金属离子; 环境化学; 水热合成

中图分类号: O613; O647.3

文献标识码: A

文章编号: 1001-4861(2020)04-0747-08

DOI: 10.11862/CJIC.2020.084

A Facile Method to Prepare Hydroxyapatite Nanotubes and Immobilization Activities Against Heavy Metal Ions in Solutions

ZOU Xue-Yan^{1,2} ZHAO Yan-Bao^{*,1,3,4} ZHANG Zhi-Jun^{*,1,2,4}

(¹Engineering Research Center for Nanomaterials, Henan University, Kaifeng, Henan 475004, China)

(²Key Laboratory for Monitor and Remediation of Heavy Metal Polluted Soils of Henan Province, Jiyuan, Henan 459000, China)

(³National & Local Joint Engineering Research Center for Applied Technology of Hybrid Nanomaterials,
Henan University, Kaifeng, Henan 475004, China)

(⁴Collaborative Innovation Center of Nano Functional Materials and Applications of Henan Province,
Henan University, Kaifeng, Henan 475004, China)

Abstract: Hydroxyapatite nanotubes (HAP NTs) were synthesized by a facile method, which were 20~40 nm in length and had a large surface area of 56 m²·g⁻¹. Then the prepared HAP NTs were employed to immobilize Pb²⁺, Cd²⁺, Cu²⁺, Co²⁺, Ni²⁺, Zn²⁺, and Hg²⁺ in aqueous solution and the as-prepared HAP NTs showed a high immobilization capacity. In addition, the desorption rate of the prepared HAP NTs on seven heavy metal ions were all less than 1%, which showed a strong stability. The experimental data was analyzed by the Langmuir and Freundlich isotherm models. The obtained results from the application of the two equations showed that the

收稿日期: 2019-08-22。收修改稿日期: 2020-02-25。

国家自然科学基金(No.21571051), 河南省重大科技专项(No.181100310600), 河南大学一流学科交叉学科建设计划(No.2019Y1XKJC04), 河南大学科研基金项目(No.2015YBZR032)和国家重点研发计划(No.2019YFC1803600)资助。

*通信联系人。E-mail: zhangzj09@126.com, zhaoyb902@henu.edu.cn

adsorption equilibrium was best fitted with a Langmuir model and monolayer adsorption capacity was $958.28 \text{ mg} \cdot \text{g}^{-1}$, which showed a perfect immobilization property. The adsorption mechanisms were further studied by energy dispersive X-ray spectrum (EDS) and X-ray diffraction (XRD) patterns and the results showed that the adsorption mechanism was the dissolution of HAP NTs and the precipitation of a more stable $\text{Pb}_5(\text{PO}_4)_3(\text{OH})$ when the amount of Pb^{2+} ions in solution was sufficient. Our study confirmed the possibilities of using HAP NTs to treat Pb-contaminated wastewater in the environmental pollution management.

Keywords: hydroxyapatite; nanotubes; immobilization; mechanism; heavy metal ions; environmental chemistry; hydrothermal synthesis

0 Introduction

With the rapid development of industries, the discharge of waste water containing heavy metals was increasing significantly. As it was well-known to all that the ingestion of heavy metals like Cd, Pb, Hg and so on could link to cancer, DNA damage or blocking of protein^[1-5]. Therefore, the remediation of heavy metals has become a hot topic. Today, many methods have been employed to remove heavy metal ions, such as chemical precipitation, adsorption, solvent extraction and coagulation^[6-11]. Among them, the chemical immobilization method was considered to be applicable to fast and large area remediation. As reported by Mirbagheri and his co-workers, $\text{Ca}(\text{OH})_2$ and NaOH were used to remove $\text{Cu}(\text{II})$ and $\text{Cr}(\text{VI})$ ions^[12]. The maximum precipitation occurred at $\text{pH}=8.7$ with the addition of $\text{Ca}(\text{OH})_2$ and the concentration of $\text{Cr}(\text{VI})$ was reduced from 30 to $0.01 \text{ mg} \cdot \text{L}^{-1}$. Özverdi et al.^[13] employed pyrite and synthetic iron sulphide to remove Cu^{2+} , Cd^{2+} and Pb^{2+} from aqueous solutions. And the adsorption of metal ions onto both adsorbents was pH-dependent and the adsorption capacities increased with the increasing temperature. With the advancement of nanotechnology, many nanomaterials were used for removing the heavy metals ions in solution. For example, ferri ferrous oxide/L-cysteine magnetic nanospheres could adsorb Pb^{2+} in aqueous solution and the maximum adsorption capacity reached to $459.33 \text{ mg} \cdot \text{g}^{-1}$, which fitted with a Langmuir model^[14].

Nevertheless, common adsorbents generally only acted on one or several heavy metal ions at the same time^[15-17]. In fact, water pollution was often caused by the coexistence of multiple heavy metal ions.

Considering the problem mentioned in the removal of many kinds of heavy metal ions, nano-hydroxyapatite was one of the most important materials in immobilizing metal ions in solution. We knew that HAP nanomaterials had a large specific surface area, which can immobilize the heavy metal ions in a high capacity through phosphate precipitation, ions exchange, surface adsorption or other mechanisms. Gómez del Río et al.^[18] employed calcite (CA) and hydroxyapatite (HAP) from minerals to study the interaction between Cd, Zn, and Co with CA and HAP. It could be seen that the affinities followed the sequence: $\text{Cd} > \text{Zn} > \text{Co}$ (CA) and $\text{Cd} > \text{Zn} \approx \text{Co}$ (HAP). Then synthetic HAP was an efficient adsorbent that has been extensively investigated for the removal of heavy metal^[19-21]. In Brasil some HAP powder samples with different crystallinity, stoichiometry, and specific surface area were prepared, which were evaluated the uptake of Cd^{2+} ions from aqueous solution. It indicated that Cd^{2+} ions sorption depended on the HAP crystallite dimensions and the major part of Cd^{2+} ions could be immobilized by the pores of HAP samples. And the influence of sample thermal treatment on Cd^{2+} ions were studied and the maximum sorption capacity decreased from 0.631 to $0.150 \text{ mmol} \cdot \text{g}^{-1}$ at 900°C ^[22]. Fuller et al gave the mechanism of $\text{U}(\text{VI})$ adsorbed by HAP, suggesting that $\text{U}(\text{VI})$ adsorbed to the HAP surfaces as an inner-sphere complex^[23]. However, HAP nanotubes (HAP NTs) has not been investigated for the removal of multi-metal (Pb^{2+} , Cd^{2+} , Cu^{2+} , Co^{2+} , Ni^{2+} , Zn^{2+} , and Hg^{2+}) from aqueous solution. And the mechanism to describe the uptake of heavy metal from aqueous solution by HAP NTs has not been extensively evaluated. In this paper, HAP NTs were

synthesized by a facile method, which had a perfect morphology in shape and a large surface area. Then the prepared HAP NTs can be used to remove seven heavy metal ions (Pb^{2+} , Cd^{2+} , Cu^{2+} , Co^{2+} , Ni^{2+} , Zn^{2+} and Hg^{2+}) in the multi-metal system. Meanwhile, the mechanism of HAP NTs on heavy metal ions was further studied.

1 Experimental

1.1 Materials

P_2O_5 (AR, 98.0%) and $\text{Ca}(\text{NO}_3)_2 \cdot 4\text{H}_2\text{O}$ (AR, 99.0%) were bought from Tianjin Kermel Chemical Reagent Company Ltd. Diethylenetriamine pentaacetic acid (DTPA, AR, 99.7%) and triethanolamine (TEA, AR, 98.0%) was purchased from Sinopharm Group Pharmaceutical Company Ltd. CaCl_2 (AR, 99.0%) was acquired from Tianjin Guangfu Fine Chemical Research Institute.

1.2 Preparation of HAP NTs

In a typical synthesis, 0.20 g of P_2O_5 was added into 15 mL of absolute ethanol, followed by the addition of the mixed solution (1.20 g of $\text{Ca}(\text{NO}_3)_2 \cdot 4\text{H}_2\text{O}$ and 15 mL of H_2O) under stirring. Then the pH value was adjusted to 8.80 by ammonia spirit (25%~28%(w/w)) and was kept at 17 °C under stirring for 30 min. Subsequently, the solution was transferred into a Teflon-lined stainless-steel autoclave, sealed and heated at 165 °C for 12 h. Finally, the solution was cooled, centrifuged and washed with ethanol and water for several times to obtain the HAP NTs.

1.3 Adsorption-desorption measurements

Briefly, 0.10 or 0.50 g of HAP NTs were dispersed in 30.00 mL of Pb^{2+} , Cd^{2+} , Cu^{2+} , Co^{2+} , Ni^{2+} , Zn^{2+} and Hg^{2+} single/mixed solution (20 $\text{mg} \cdot \text{L}^{-1}$ for each ion) by stirring at 180 $\text{r} \cdot \text{min}^{-1}$ at room temperature for 20 min. In order to search the effect of adsorption time, 0.10 g of HAP NTs were dispersed in 30.00 mL of Pb^{2+} , Cd^{2+} , Cu^{2+} , Co^{2+} , Ni^{2+} , Zn^{2+} and Hg^{2+} mixed solution (20 $\text{mg} \cdot \text{L}^{-1}$ for each ion) by stirring at room temperature for a predetermined time interval (20, 40, 60, 80, 100, 120 min). Then all the precipitate were collected and washed with 10 mL water to remove M^{2+} ions physically adsorbed.

Meanwhile, another 10 mL water was added. After 1 h, the supernatant was collected and the above operation was repeated 12 times. Different amount of HAP NTs (0.02, 0.04, 0.06, 0.08 g) was dispersed in 30 mL of Pb^{2+} solution (1 000 $\text{mg} \cdot \text{L}^{-1}$) under stirring at room temperature for 2 h. The concentrations of heavy metal ions in the supernatant was analyzed by inductively coupled plasma (ICP).

1.4 Mechanism of HAP NTs immobilizing on seven metal ions

In a typical method, 0.1 g of HAP NTs were dispersed into different volumes (10, 20, 30, 40, 50, 60 mL) of Pb^{2+} , Cd^{2+} , Cu^{2+} , Co^{2+} , Ni^{2+} , Zn^{2+} and Hg^{2+} mixed solution (1 000 $\text{mg} \cdot \text{L}^{-1}$ for each ion). Then these solutions were shaken for 24 h at room temperature (180 $\text{r} \cdot \text{min}^{-1}$). After adsorption, these HAP/M precipitate ($\text{M}=\text{Pb}$, Cd , Cu , Co , Ni , Zn , Hg) were collected and dried at 60 °C for 24 h.

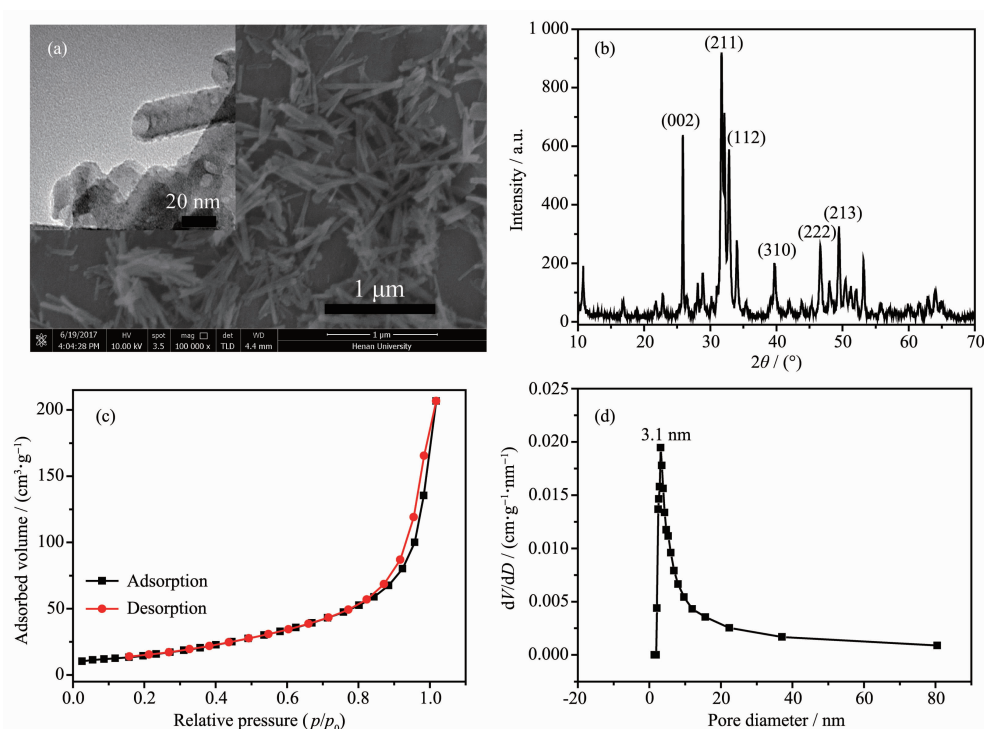
1.5 Characterization

X-ray diffraction (XRD) measurements were carried out on an D8-ADVANCE X-ray diffraction spectrometer (XRD, Bruker, Germany) with a $\text{Cu } K\alpha$, $\lambda=0.154$ 18 nm radiation ($U=60$ kV, $I=60$ mA) at scan rate of $0.04^\circ \cdot \text{s}^{-1}$ in a region of 2θ from 10° to 70° . The morphology of HAP NTs was analyzed by transmission electron microscopy (TEM, JEM-2010, Japan, working at 200 kV) and scanning electron microscopy (SEM, JSM5600LV, Japan, 5 kV, 10 mA). To explore the surface area, cumulative pore volume and pore size distribution of HAP NTs, the Brunauer-Emmett-Teller method (BET, QUADRASORB, USA) were employed and determined at 77 K. The concentration of heavy metal ions were measured by ICP (Optima 2100DV, USA).

2 Results and discussion

2.1 Characterization of HAP NTs

Fig.1a was the TEM and SEM images of the HAP NTs. It was seen that the synthesized HAP sample was tube-like shape, 20~40 nm in diameter and 145~750 nm length with aspect ratio ranging from 5 to 13. We observed the detailed morphology of the nanotubes in Fig.1a (insert), which had a porous surface texture.



Inset in Fig.1a showed the TEM image

Fig.1 SEM image (a), XRD pattern (b), N_2 adsorption-desorption isotherm (c) and pore diameter distribution (d) of the prepared HAP samples

And we can see that the inner diameter of the prepared HAP nanotubes was about 7.6 nm. The presence of numerous individual small white dots obviously suggested the existence of mesopores (4~5.5 nm), spreading around the surfaces of HAP NTs, which was in agreement with the literature^[24]. Fig.1b showed the XRD pattern of the HAP NTs. The XRD patterns showed a strong peak at around 31.7° corresponding to (211) the planes of HAP crystalline structure and the other characteristic peaks were from (002), (112), (310), (222) and (213) planes, respectively. These characteristic peaks in the pattern of the prepared HAP NTs agreed well with the standard pattern (PDF No.09-0432). The N_2 adsorption and desorption isotherm of prepared HAP were shown in Fig.1c. It was seen that the isotherm of the sample showed the typical IV adsorption isotherm with a distinct hysteresis loop. The BET surface area of the sample was $56 \text{ m}^2 \cdot \text{g}^{-1}$, which had a larger surface area^[15,25-26]. It was clear that the HAP NTs presented narrow pore diameter distribution, and the pore diameter was mainly focused on 3 nm.

2.2 Immobilization property of HAP NTs on seven heavy metal ions

Fig.2a was the immobilization rate of HAP NTs on Pb^{2+} , Cd^{2+} , Cu^{2+} , Co^{2+} , Ni^{2+} , Zn^{2+} and Hg^{2+} in single ion solution ($20 \text{ mg} \cdot \text{L}^{-1}$ for each ion). We observed that the immobilization rate was nearly 100%, which showed that HAP NTs had a strong adsorption property. In order to verify the effect of multiple ions, we simultaneously adsorbed seven mixed ions of the same concentration. It can be seen in Fig.2b that the immobilization rate was 100% (Pb^{2+}), 100% (Cd^{2+}), 100% (Cu^{2+}), 99.92% (Zn^{2+}), 99.85% (Co^{2+}), 99.32% (Hg^{2+}) and 98.78% (Ni^{2+}), respectively, which also showed a perfect immobilizing property to seven mixed ions. Fig.2c was the relationship between the immobilization rate and immobilization time of the HAP NTs. From the Fig.2c we noticed that the immobilization rate for each heavy ion reached 100% in 20 min, which indicated that HAP NTs had a rapid adsorption reaction with heavy metal ions. In order to verify the stability of HAP NTs adsorbed the target heavy metal ions, we conducted a continuous 12 h

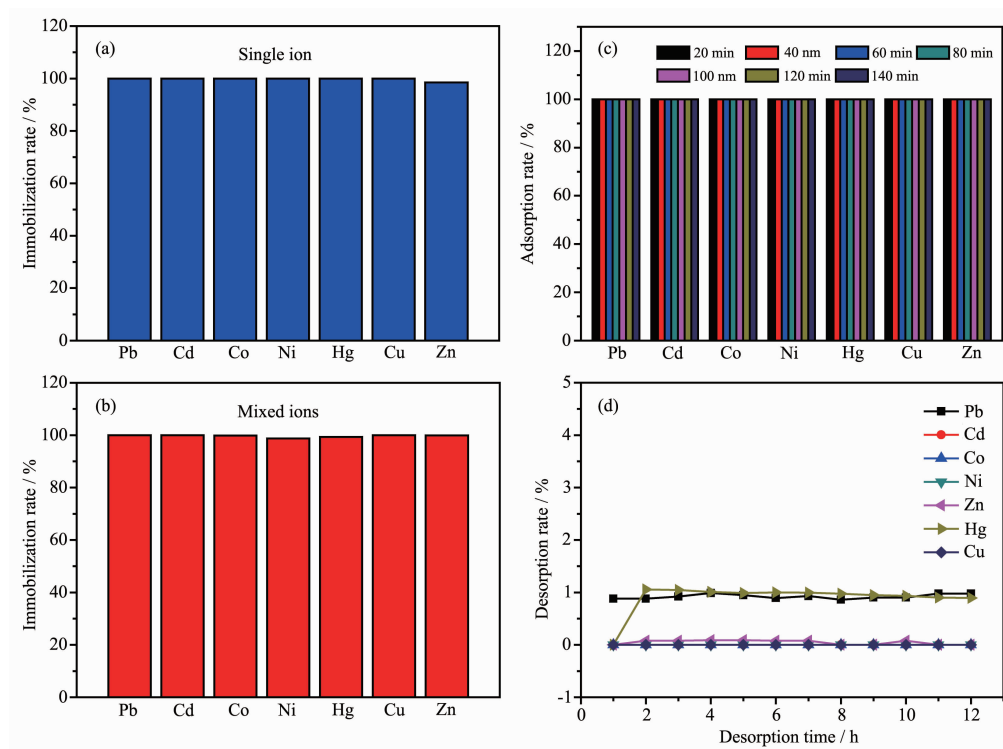


Fig.2 Immobilization rate of HAP NTs on single ions (a) and mixed ions (b); Adsorption time (c) and desorption rate (d) of HAP NTs on mixed ions

desorption experiment. It was seen that the desorption rate of seven metal ions was less than 1%, which showed a strong stability (Fig.2d).

2.3 Heavy metal uptake mechanism

Fig.3a and 3b were the EDS pattern of HAP/M obtained in 10 and 60 mL mixed ions solution. Table 1 was the atom percent from EDS of HAP/M obtained in different amounts of mixed ions solution. It could be seen from EDS pattern that there were Pb, Cd, Cu, Co, Ni, Zn and Hg elements in HAP/M, indicating that seven heavy metal ions had been immobilized by the prepared HAP NTs. Nevertheless, there were obvious

differences between Fig.3a and 3b. When the amount of seven metal ions was less than 30 mL, the peak of Ca element was stronger than that of Pb element. However, when the amount of seven metal ions was more than 30 mL, it can be seen that the peak of Pb element in Fig.3d became stronger. This could be happened as the immobilization occurred via the surface complexation immobilized a little amount of metal ions, whereas immobilization through ion exchange with Ca^{2+} ions in the lattice and heavy metals ions could immobilize a sufficient amount of heavy metal ions^[19].

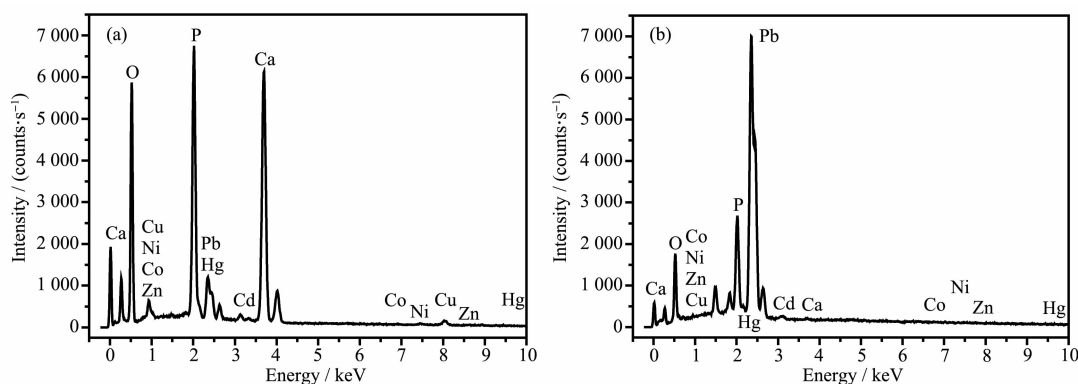


Fig.3 EDS of HAP/M obtained in 10 (a) and 60 mL (b) mixed ions solution

Table 1 Atomic fraction from EDS of HAP/M obtained in 10~60 mL mixed ions solution

Volume / mL	Atomic fraction / %			
	Ca	P	O	Pb
10	12.75	8.99	74.71	0.8
20	15.08	11.29	67.32	4.01
30	11.80	9.46	73.67	4.52
40	13.65	10.58	69.79	4.24
50	8.35	6.93	75.45	4.49
60	9.03	7.66	75.34	5.21

In order to verify the component of HAP/M, the relationship between the molar ratio of M to P of HAP/M and different amount of mixed ions solution were given in Fig.4. It was seen that the molar ratio of Ca to P of HAP/M went down from 1.42:1 to 1.18:1 with the increase of the adding volume of mixed ions solution, less than that of HAP (1.67:1). It was indicated that there was an ion exchange reaction between Ca^{2+} ions in HAP and heavy metal ions. Meanwhile, we also observed that among the seven heavy metal elements, the content of Pb element was the highest and the atomic percentage of Pb in HAP/M reached by 5.21% (Table 1). As was well-known, the solubility product constant (K_{sp}) was the equilibrium constant for a chemical reaction in which a solid ionic compound dissolved to yield its ions in solution. It may be because the K_{sp} of $\text{Pb}_3(\text{PO}_4)_2$ was 8.0×10^{-43} , which was far less than that of $\text{Ca}_3(\text{PO}_4)_2$ (2.07×10^{-33}). When the concentration of Pb^{2+} ions in mixed solution was sufficient enough, Pb^{2+} can exchanged with Ca^{2+} to form $\text{Pb}_5(\text{PO}_4)_3(\text{OH})$. Meanwhile,

we all knew that $\text{Pb}_5(\text{PO}_4)_3(\text{OH})$ was extremely stable and insoluble, which showed consistency with the results of desorption experiment in Fig.2d.

In order to verify the component of the obtained HAP/M, XRD analysis was employed. Fig.5 was the XRD patterns of the HAP/M obtained in different amounts (10~60 mL) of mixed ions solution. From Fig. 5, curve 1~3, it was seen that the HAP/M presented characteristic peaks at 25.88° (002), 31.77° (211), 32.20° (112), 39.82° (310) and 46.71° (222), consistent with the standard card of HAP (PDF No.09-0432). At the same time, five intent peaks at 2θ of 21.60° , 26.11° , 30.02° , 31.90° and 44.01° were indexed to scattering from the (111), (102), (112), (202) and (222) crystal planes of the $\text{Pb}_5(\text{PO}_4)_3(\text{OH})$ (PDF No.24-0586), respectively. It was indicated that the component of HAP/M was the mixture of HAP and $\text{Pb}_5(\text{PO}_4)_3(\text{OH})$ when the amount of M^{2+} solution was less than 30 mL. At this point, the immobilization mechanism between HAP NTs and heavy metal ions was mainly rapid

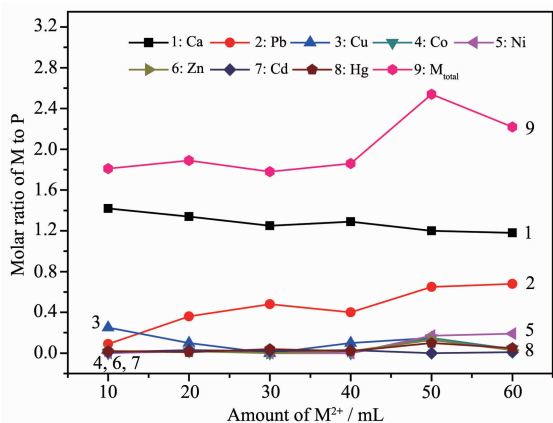
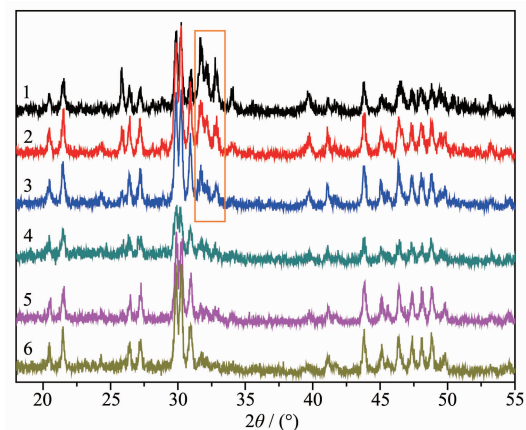


Fig.4 Relationship between the ratio of M to P of HAP/M and different amounts of mixed ions solution



1: 10 mL; 2: 20 mL; 3: 30 mL; 4: 40 mL; 5: 50 mL; 6: 60 mL

Fig.5 XRD patterns of HAP/M obtained in different amounts of mixed ions solution

surface complexation and there was a little ion exchange resulting in partial dissolution of HAP^[19]. When the adding volume of mixed ions solution was more than 40 mL, we can see that the component of HAP/M was changed into $\text{Pb}_5(\text{PO}_4)_3(\text{OH})$ (PDF No.24-0586), seen in Fig.5, curve 4~6. This indicated that when Pb^{2+} ions in the solution reached a certain amount, Pb^{2+} ions in the solution could exchange with Ca^{2+} ions in HAP NTs, thus forming a more stable $\text{Pb}_5(\text{PO}_4)_3(\text{OH})$ ^[27], which showed consistency with the results of EDS analysis in Fig.3. At this time, the ion exchange reaction was the main mechanism between HAP NTs and heavy metal ions. This was because that Ca^{2+} in the HAP NTs sample can easily be exchanged for Pb^{2+} and the HAP can be converted into stable $\text{Pb}_5(\text{PO}_4)_3(\text{OH})$, which was consistent with the result of the literature^[28-29].

Heavy metal immobilization by HAP NTs was analyzed using the Langmuir model and Freundlich model, which were popular isotherm models due to their simplicity. The Langmuir model was based on the assumption that the maximum adsorption occurred when a saturated monolayer of solute molecules was presented on the adsorbent surface, the energy of adsorption was constant, and there was no migration of adsorbed molecules in the plane of the surface^[30]. Freundlich model was applied to describe a heterogeneous system characterized by a heterogeneity factor of $1/n$ ^[31]. This model described reversible adsorption and was not restricted to the formation of the monolayer. The Langmuir (1) and Freundlich (2) equilibrium equation were:

$$\frac{C_e}{Q_e} = \frac{1}{Q_m} C_e + \frac{1}{bQ_m} \quad (1)$$

$$\ln Q_e = \frac{1}{n} \ln C_e + \ln k \quad (2)$$

Where C_e was the equilibrium concentration of aqueous Pb^{2+} ions ($\text{mg} \cdot \text{L}^{-1}$); Q_e was the amount of Pb^{2+} sorbed per gram of HAP NTs ($\text{mg} \cdot \text{g}^{-1}$); Q_m related to the maximum sorption capacity ($\text{mg} \cdot \text{g}^{-1}$); b was the Langmuir constant ($\text{L} \cdot \text{mg}^{-1}$); $1/n$ was the the degree of non linearity between solution concentration and adsorption; k was the Freundlich isotherm constant ($\text{mg}^{1-\frac{1}{n}} \cdot \text{L}^{\frac{1}{n}} \cdot \text{g}^{-1}$)^[14].

Fig.6 showed typical sorption isotherms for Pb-adsorbent systems, which listed the isotherm fitted equation and correlation coefficients calculated based on Langmuir and Freundlich models. It could be seen that the fitting equilibrium adsorption data of Pb^{2+} with the Langmuir isotherm model provided an extremely high correlation coefficient of $R^2=0.999\ 9$, higher than $0.913\ 9$ derived from the Freundlich model. This suggested that adsorption of Pb^{2+} by HAP NTs was monolayer-type, which was in accordance with the general observation that adsorption from an aqueous solution usually formed a layer on the sorbed surface. Besides, the Q_m value of the HAP NTs adsorbent, calculated from the Langmuir isotherm model, was as much as $980.39\ \text{mg} \cdot \text{g}^{-1}$, which was consistent with the experimental data ($958.28\ \text{mg} \cdot \text{g}^{-1}$) and showed a perfect immobilization property. It showed that the Q_m value of the HAP NTs adsorbent in this study were significantly higher than the reported adsorbents^[21,32-33]. The Langmuir parameters indicated that the HAP NTs

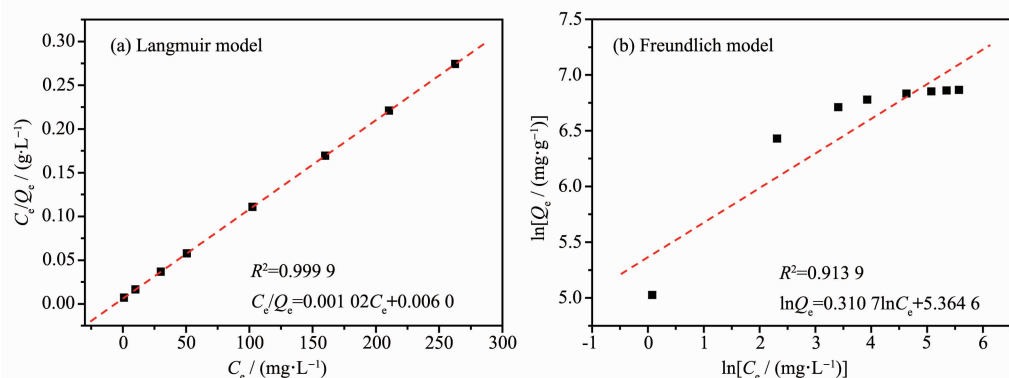


Fig.6 Langmuir and Freundlich isotherms for HAP NTs on Pb^{2+}

were a suitable adsorbent for the adsorption of heavy metal ions from aqueous solution.

3 Conclusions

Hydroxyapatite nanotubes with controllable morphology were synthesized by a facile method. The prepared HAP nanotubes could rapidly and effectively immobilize seven heavy metal ions (Pb^{2+} , Cd^{2+} , Cu^{2+} , Co^{2+} , Ni^{2+} , Zn^{2+} and Hg^{2+}) at the same time. Meanwhile, the as-prepared HAP NTs showed a fast adsorption rate, a high immobilization capacity and a strong stability, which had potential application prospects in mitigating water/soil pollution.

Acknowledgements: The authors acknowledge the financial support provided by the National Natural Science Foundation of China (Grant No.21571051), the Major Science and Technology Project of Henan Province (Grant No. 181100310600), the Interdisciplinary Research for First-class Discipline Construction Project of Henan University (Grant No. 2019YLXKJC04), the Scientific Research Fund Project of Henan University (Grant No.2015YBZR032), and National Key Research and Development Program of China (Grant No. 2019YFC1803600).

References:

- [1] Bastaa N T, McGowen S L. *Environ. Pollut.*, **2004**,**127**(1):73-82
- [2] Zhang X L, Zhao X L, Li B Z, et al. *Chinese Sci. Bull.*, **2014**,**59**(25):3134-3141
- [3] Ling W T, Shen Q, Gao Y Z, et al. *Aust. J. Soil Res.*, **2007**, **45**(8):618-623
- [4] Tan J J, He S B, Yan S H, et al. *Protoplasma*, **2014**,**251**(5): 1213-1221
- [5] Xiao T W, Mi M M, Wang C Y, et al. *Environ. Exp. Bot.*, **2018**,**153**:45-53
- [6] Li J, Chen C L, Zhu K R, et al. *J. Taiwan Inst. Chem. Eng.*, **2016**,**59**:389-394
- [7] Mahajan G, Sud D. *Pol. J. Chem. Technol.*, **2014**,**16**:6-13
- [8] Singh P K, Wang W J, Shrivastava A K. *Aquat. Toxicol.*, **2018**,**202**:36-45
- [9] Kapur M, Mondal M K. *Desalin. Water Treat.*, **2016**,**57**(27): 12620-12631
- [10] Zhang P, Wang R L, Ju Q, et al. *Plant Physiol.*, **2019**,**180** (1):529-542
- [11] Ponder S M, Darab J G, Mallouk T E. *Environ. Sci. Technol.*, **2000**,**34**(12):2564-2569
- [12] Mirbagheri S A, Hosseini S N. *Desalination*, **2005**,**171**(1):85-93
- [13] Özverdi A, Erdem M. *J. Hazard. Mater.*, **2006**,**137**(1):626-632
- [14] Zou X Y, Yin Y B, Zhao Y B, et al. *Mater. Lett.*, **2015**,**150**: 59-61
- [15] Xiong L, Chen C, Chen Q, et al. *J. Hazard. Mater.*, **2011**, **189**(3):741-748
- [16] Ponder S M, Darab J G, Mallouk T E. *Environ. Sci. Technol.*, **2000**,**34**(12):2564-2569
- [17] Kanel S R, Manning B, Charlet L, et al. *Environ. Sci. Technol.*, **2005**,**39**(5):1291-1298
- [18] Gómez del Río J A, Morando P J, Cicerone D S. *J. Environ. Manage.*, **2004**,**71**:169-177
- [19] Corami A, Mignardi S, Ferrini V. *J. Hazard. Mater.*, **2007**, **146**(1/2):164-170
- [20] Zou X Y, Zhao Y B, Zhang Z J. *J. Contam. Hydrol.*, **2019**, **226**:103538-103544
- [21] Tang W Q, Zeng R Y, Feng Y L, et al. *Chem. Eng. J.*, **2013**, **223**:340-346
- [22] Da Rocha N C C, De Campos R C, Rossi A M, et al. *Environ. Sci. Technol.*, **2002**,**36**(7):1630-1635
- [23] Fuller C C, Bargar J R, Davis J A, et al. *Environ. Sci. Technol.*, **2002**,**36**(2):158-165
- [24] Zhang C M, Li C X, Huang S S, et al. *Biomaterials*, **2010**,**31** (12):3374-3383
- [25] Sneha M, Meenakshisundaram N, Kandaswamy A. *Bull. Mater. Sci.*, **2016**,**39**(2):509-517
- [26] Lin K L, Pan J Y, Chen Y W, et al. *J. Hazard. Mater.*, **2009**, **161**(1):231-240
- [27] Manecki M, Maurice P, Traina S J. *Soil Sci.*, **2000**,**165**(12): 920-933
- [28] Jeanjean J, Vincent U, Fedoroff M. *J. Solid State Chem.*, **1994**,**108**(1):68-72
- [29] Suzuki T, Ishigaki K, Miyake M. *J. Chem. Soc., Faraday Trans. 1*, **1984**,**80**(11):3157-3165
- [30] Kumar R, Bishnoi N R, Nagpal G, et al. *Chem. Eng. J.*, **2008**,**135**(3):202-208
- [31] Albadarin A B, Mangwandi C, Al-Muhtaseb A, et al. *Chem. Eng. J.*, **2012**,**179**:193-202
- [32] Jain M, Garg V K, Kadirvelu K. *J. Hazard. Mater.*, **2009**, **162**(1):365-372
- [33] De Lima L S, Araujo M D M, Percio S, et al. *Chem. Eng. J.*, **2011**,**166**(3):881-889